A Novel Method to Capture the Onset of Dynamic Electrocardiographic Ischemic Changes and its Implications to Arrhythmia Susceptibility

Omid Sayadi, Dheeraj Puppala, Nosheen Ishaque, Rajiv Doddamani, Faisal M. Merchant, Conor Barrett, Jagmeet P. Singh, E. Kevin Heist, Theofanie Mela, Juan Pablo Martínez, Pablo Laguna and Antonis A. Armoundas

J Am Heart Assoc. 2014;3:e001055; originally published September 3, 2014;
doi: 10.1161/JAHA.114.001055
The *Journal of the American Heart Association* is published by the American Heart Association, 7272 Greenville Avenue, Dallas, TX 75231
Online ISSN: 2047-9980

ORIGINAL RESEARCH

A Novel Method to Capture the Onset of Dynamic Electrocardiographic Ischemic Changes and its Implications to Arrhythmia Susceptibility

Omid Sayadi, PhD; Dheeraj Puppala, MD; Nosheen Ishaque, MD; Rajiv Doddamani, MD; Faisal M. Merchant, MD; Conor Barrett, MD; Jagmeet P. Singh, MD, PhD; E. Kevin Heist, MD, PhD; Theofanie Mela, MD; Juan Pablo Martínez, PhD; Pablo Laguna, PhD; Antonis A. Armoundas, PhD

***Background*—**This study investigates the hypothesis that morphologic analysis of intracardiac electrograms provides a sensitive approach to detect acute myocardial infarction or myocardial infarction-induced arrhythmia susceptibility. Large proportions of irreversible myocardial injury and fatal ventricular tachyarrhythmias occur in the first hour after coronary occlusion; therefore, early detection of acute myocardial infarction may improve clinical outcomes.

***Methods and Results*—**We developed a method that uses the wavelet transform to delineate electrocardiographic signals, and we have devised an index to quantify the ischemia-induced changes in these signals. We recorded body-surface and intracardiac electrograms at baseline and following myocardial infarction in 24 swine. Statistically significant ischemia-induced changes after the initiation of occlusion compared with baseline were detectable within 30 seconds in intracardiac left ventricle ($P<0.0016$) and right ventricle–coronary sinus ($P<0.0011$) leads, 60 seconds in coronary sinus leads ($P<0.0002$), 90 seconds in right ventricle leads ($P<0.0020$), and 360 seconds in body-surface electrocardiographic signals ($P<0.0022$). Intracardiac leads exhibited a higher probability of detecting ischemia-induced changes than body-surface leads ($P<0.0381$), and the right ventricle–coronary sinus configuration provided the highest sensitivity (96%). The 24-hour ECG recordings showed that the ischemic index is statistically significantly increased compared with baseline in lead I, aVR, and all precordial leads ($P<0.0388$). Finally, we showed that the ischemic index in intracardiac electrograms is significantly increased preceding ventricular tachyarrhythmic events ($P<0.0360$).

***Conclusions*—**We present a novel method that is capable of detecting ischemia-induced changes in intracardiac electrograms as early as 30 seconds following myocardial infarction or as early as 12 minutes preceding tachyarrhythmic events. **(*J Am Heart Assoc*. 2014;3:e001055 doi: 10.1161/JAHA.114.001055)**

Key Words: ECG delineation • intracardiac signals • ischemic index • myocardial infarction • wavelet transform

From the Division of Cardiology, Massachusetts General Hospital, Harvard Medical School, Boston, MA (O.S., D.P., N.I., R.D., A.A.A); Cardiology Division, Emory University School of Medicine, Atlanta, GA (F.M.M); Division of Cardiology, Cardiac Arrhythmia Service, Massachusetts General Hospital, Boston, MA (C.B., J.P.S., E.K.H., T.M.); Biomedical Signal Interpretation & Computational Simulation (BSICoS) Group, Aragon Institute of Engineering Research, IIS Aragón, University of Zaragoza, Zaragoza, Aragon, Spain (J.P.M., P.L.); Centro de Investigación Biomédica en Red en Bioingeniería, Biomateriales y Nanomedicina (CIBER-BBN), Zaragoza, Aragon, Spain (J.P.M., P.L.).

Correspondence to: Antonis A. Armoundas, PhD, Cardiovascular Research Center, Massachusetts General Hospital, 149 13th Street, Charlestown, MA 02129. E-mail: aarmoundas@partners.org

Received May 5, 2014; accepted June 3, 2014.

Myocardial ischemia (MI) may establish the substrate for fatal ventricular tachyarrhythmic events (VTEs) both acutely and over the long term.[1,2] Early diagnosis and risk stratification of patients with acute MI is essential to guide prompt intervention and optimal clinical outcome.

Electrocardiographic ST-segment monitoring has been used widely to detect acute MI.[3,4] In the standard 12-lead ECG, ST-segment deviation is the most common determinant of ongoing ischemia[5,6] and a strong predictor of associated mortality.[7] Sensitivity in detecting acute MI, however, remains inadequately low.[8–10] Whether it is due to the variability of the ischemia-induced changes in various ECG leads, as shown by body-surface potential mapping[11] or the inaccuracy in detecting the elevated J-points,[12] body-surface ECGs may not reveal subendocardial[13] and even severe transmural ischemia.[14]

With the advent of the implantable cardioverter defibrillator, defibrillation of ventricular tachyarrhythmias has resulted in significant improvements in survival.[15] Recent evidence

also suggests that continuous monitoring of a patient's ST-segment changes in intracardiac electrograms may allow an implanted device to detect acute closure of a coronary artery that could lead to a reduction in symptom-to-door time and thereby potentially improve clinical outcomes.[16] Furthermore, it has been shown recently that the high-risk period for sudden death of patients who survive acute MI extends beyond the hospitalization period, mostly due to recurrent MI or extension of the infarcted area.[1,2]

The preceding data provide strong evidence that early detection of MI, in either the ambulatory ECG or from an implantable device, is of significant therapeutic potential in high-risk patients. This study investigates the hypothesis that early onset of MI may be captured through a novel method that is based on a robust ECG delineator that accurately estimates the MI-induced depolarization and repolarization changes and that those changes are more prominent in intracardiac leads. We probed this hypothesis in a swine model of acute MI and developed an algorithm for body-surface and intracardiac electrograms to quantify changes of the depolarization phase as well as the ST segment before and after ischemia induction.

Methods

Animal Preparation

The animal studies were approved by the institutional review board and the subcommittee on research animal care at Massachusetts General Hospital.

The total study population comprised 24 male Yorkshire swine (40 to 45 kg) that were anesthetized and instrumented in the Animal Electrophysiology Laboratory at Massachusetts General Hospital, as described previously.[17] Each animal was intubated and placed on a mechanical ventilator, and anesthesia was maintained with isoflurane (1.5% to 2.5%).

Standard ECG electrodes were placed on the animal's limbs and chest. For intracardiac recording, percutaneous vascular access was obtained in the jugular veins and femoral arteries and veins using standard Seldinger techniques.[18] Decapolar catheters were placed under fluoroscopic guidance in the right atrium, right ventricle (RV), coronary sinus (CS), and left ventricle (LV). An inferior vena cava catheter was inserted as a reference electrode for unipolar signals. An arterial line was used to monitor invasive blood pressure. Regional MI was induced by balloon occlusion of the proximal left circumflex coronary artery, using standard percutaneous cardiac catheterization techniques. Ischemia was validated and confirmed by hand injections of contrast into the coronary, in which case no-flow as well as electrocardiographic changes were indications of full occlusion. In 4 animals, 24-hour Holter ECG recordings were performed before and immediately after MI.

Equipment and Data Collection

Two standard body-surface signals (leads II and V4) and 12 intracardiac unipolar electrocardiographic signals (from the CS, LV, and RV catheters) were recorded through a Prucka Cardiolab (GE Healthcare) electrophysiology system and digitized at a sampling rate of 1 kHz by a multichannel 16-bit data acquisition card (M-Series PCI-6255; National Instruments). The Prucka system provided 16 high-fidelity analog output signals with front-end signal conditioning as well as isolation protection of the signal-analysis system from defibrillation. Intracardiac electrograms were band-pass filtered 0.05 to 500 Hz, with 60-Hz notch filter and gain 250 V/V, and body surface signals were band-pass filtered 0.05 to 100 Hz, with 60-Hz notch filter and gain 2500 V/V, as described previously.[17] Data analysis was performed using custom-written software in MATLAB (MathWorks Inc).

ECG Delineation Using Established Methods

We have implemented 4 commonly used threshold-based methods to detect the onset and offset of ECG waveforms. Prior to application of each method, a linear baseline adjustment was performed for each beat. The methods are as follows:

1. *Waveform*: determines the onset and offset points at times corresponding to 5% and 95% of the maximum normalized amplitude.[19]
2. *Power*: identifies the onset and offset points at time bins corresponding to 5% and 95% of the cumulative sum of the signal power.[20]
3. *Absolute*: is similar to the second approach except the threshold is applied to the cumulative sum of the absolute value of the signal.[19,21]
4. *Noise*: estimates the standard deviation (SD) of a predefined window (the noise window) of the baseline adjusted waveform and determines the onset and offset points at times when the signal exceeds 3 times the SD of the signal in the noise window.[22]

ECG Delineation Using the Wavelet Transform

To overcome potential limitations of the established ECG delineation methods, we sought to develop a method that would prove robust in determining the complex annotations of intracardiac electrograms.

The wavelet transform (WT) offers simultaneous interpretation of the signal in both time and frequency using a frequency-dependent window that allows high localization in time for high-frequency signal components as well as high-frequency resolution for low-frequency patterns (multi-resolution analysis). The WT decomposes the signal as a

combination of a set of basis functions obtained by means of dilation and translation of a single prototype wavelet. In this time-resolution description of the signal, higher frequency components are characterized by the coefficients corresponding to narrower basis functions resulting from lower scale factors and vice versa.[23]

We have developed an intracardiac ECG delineation algorithm based on a previously developed method for body-surface ECG delineation using the WT.[24] The algorithm starts with obtaining R-wave annotations through a 2-step process of first identifying the R wave using a QRS detector and then refining the R-wave location using cross-correlation, as described previously.[17] Then, for each beat, the dyadic WT of the signal is estimated for the first 5 scales, wherein most of the energy of the signal lies. A quadratic spline is used as prototype wavelet that corresponds to a derivative of a low-pass smoothing function. This ensures that the wavelet coefficients are proportional to the derivative of the filtered version of the signal with a smoothing impulse response at each scale.[23] This approach allows the identification of significant points in the ECG signal using the information of local maxima, minima, and zero crossings of the WT coefficients at different scales.

Once WT coefficients are estimated, a search window relative to the R wave and depending on the RR interval is defined. The number and polarity of the maximum modulus of WT within this window and across different scales reflects the characteristic points corresponding to ECG waveforms.[24] To accommodate the delineation of intracardiac signals, that algorithm[24] was modified to start with scale 2^3 for P-wave and T-wave delineation. Moreover, we devised reduced amplitude thresholds proportional to the root-mean-square value of the WT at the corresponding scales. To accommodate the loss of time resolution in the growing scales, we devised a multiscale approach for P-wave, QRS, and T-wave delineation; therefore, if a waveform boundary is not found in a specific scale, we repeat the above process over higher scales.

Ischemic Marker of Intracardiac and Body Surface Electrocardiographic Data

ST-segment changes have been well established as strong predictors of acute MI[1,3–5] and VTEs.[25] Also, several studies have reported changes in the depolarization phase following acute MI, in both animals[26,27] and humans.[28,29]

We devised an index that reflects MI-induced changes of both ventricular depolarization and repolarization on a beat-to-beat basis. The ischemic index is estimated as the absolute value of the ratio of ST height to the amplitude of QR, where ST height is defined as the mean ST amplitude over all points from QRS offset to T-wave onset that are greater (ST elevation) or smaller (ST depression) than the isoelectric baseline.[30] If the amplitude of the signal at QRS offset has opposite polarity with that at T-wave onset, then we choose the longer segment (in the QRS offset to T-wave onset interval) to estimate the ST height. Thus, the ischemic index is independent of a lead-by-lead variability of the signal amplitude.

A 4-step procedure was applied to compute the ischemic index. First, preliminary R-wave peaks were obtained by applying a software-based QRS detection algorithm to a body surface or intracardiac lead. Then, for each lead, initial QRS detections were refined using a template-matching QRS alignment algorithm,[17] and abnormal beats (ie, premature ventricular complexes and aberrantly conducted beats) were identified and excluded. The third step consisted of determining the ECG waveform annotations of each beat using the WT delineator. The characteristic points and waveform boundaries were independently determined using the WT-based technique for the body-surface, intracardiac unipolar leads, and intracardiac far-field bipolar leads, individually. In all leads, the isoelectric baseline was measured as the interval following the P wave and preceding the QRS_{onset}. Because this interval in CS leads is not flat, the interval following the T wave and preceding the next P wave was considered as the isoelectric baseline in these leads. Finally, the ischemic index was estimated for each beat using the aforementioned definition.

Statistical Analysis

Our results are presented as mean±SE for continuous variables. The duration of the recording and mean heart rate in each data set were compared before and after coronary artery occlusion using the Wilcoxon matched-pairs signed-rank test. Comparison of the percentage of premature ventricular complexes before and after coronary artery occlusion was performed using a generalized linear model with repeated measurements and fitting this model using a generalized estimating equation method. Bland-Altman agreement analysis was performed for all ECG leads together, and the mean difference and the limits of agreement were used to evaluate degree of agreement between the automated point annotation and the manual reference. We used a paired nonparametric Wilcoxon signed-rank test to evaluate the changes in the ischemic index from baseline to subsequent measurements. Bonferroni correction was used to adjust the significance level for multiple comparisons. Comparisons between probabilities of detecting a significant change across catheters was performed using Kruskal-Wallis analysis of variance. Ischemic index changes from baseline to 24 hours after MI were analyzed using linear mixed-effects models with random subject intercepts to account for repeated measures. A univariate autoregressive model was used for dynamic regression to describe time-dependent changes of ischemic

index at baseline and after MI until sudden cardiac death. Statistical analysis was performed using MATLAB and Stata (StataCorp LP).

Results

Detailed description of the subjects involved in the study is provided in the Table.

Evaluation of the ECG Delineation

Two expert reviewers provided manual annotations of P_{onset}, P_{offset}, QRS_{onset}, QRS_{offset}, T_{onset}, and T_{offset}. The manual annotations were used as the gold standard for evaluating each of the delineation methods. Specifically, for each subject, 200 baseline and 200 postocclusion beats of 2 body-surface, 3 CS, 4 LV, and 5 RV leads were given to 2 independent trained individuals. We developed a graphical user interface to display high-resolution ECG beats and to provide a custom-designed delineation tool that allowed the user to annotate the waveform of the ECG. Finally, the reference manual waveform annotations for each beat were estimated as the average of the annotations provided by the 2 reviewers.

Figure 1 shows representative examples of body-surface and unipolar intracardiac electrograms obtained before and after coronary artery occlusion. For each beat, the manual annotations (vertical lines) and the wavelet-based delineation results (circles) are also provided.

We evaluated the accuracy of all 5 delineation methods at baseline and after coronary artery occlusion, compared with the manual annotations, in both body-surface and intracardiac leads. Figure 2 shows the difference between the automatic annotations obtained by each method and the average of the 2 sets of manual annotations for each ECG waveform. Linear regression (each algorithm versus manual annotation) using all waveform annotations showed that wavelet-based delineations provide the closest estimation to the manual annotations both at baseline and after coronary artery occlusion. Notably, the difference in the non–wavelet-based methods is more pronounced for points involving the ST segment (ie, QRS offset and T-wave onset), most likely due to the pronounced changes in that portion of the ECG waveform occurring during acute MI.

To assess the degree of agreement between each of the automated methods and the manual annotations, we used the Bland-Altman approach to estimate the mean difference and the SD of differences among all beat annotations (6 annotations per beat) across all subjects. The mean difference and the limits of agreement (defined as twice the SD of differences) were estimated for wavelet, waveform, power, absolute, and noise methods, respectively, at baseline as 8.65±2.37, 50.61±10.26, 27.10±9.49, 38.50±8.38, and 48.08±9.71 ms and following coronary artery occlusion as 9.45±5.55, 46.40±12.71, 27.30±8.48, 38.47±11.31, and 43.14±12.34 ms. The mean differences as well as the margins of agreement for wavelet annotations are small enough and indicative that WT most closely identifies manually determined ECG time bins at baseline and following balloon occlusion.

Intra- and Intersubject Variability Analysis of Ischemic Index

Having established the WT as a robust method to accurately assess the ECG delineation of body-surface and intracardiac electrograms, we sought to examine the ability of this method to capture subtle electrogram changes underlying an abnormal electrophysiological substrate. Consequently, we evaluated the hypothesis that the proposed ischemic index that

Table. Study Population Characteristics

Study	Measures	Baseline	Post-MI	*P* Value
Acute MI	Number of records	17	17	—
	Heart rate (bpm)	109.36±12.98	110.72±16.09	0.65
	PVC occurrence (%)	0.98±1.34	0.82±1.01	0.63
Pre-VTE	Number of records	9	9	—
	Heart rate (bpm)	111.90±15.55	106.05±8.26	0.25
	PVC occurrence (%)	0.59±0.68	1.44±2.38	0.19
Holter	Number of records	4	4	—
	Heart rate (bpm)	112.70±7.31	151.01±22.42	0.12
	PVC occurrence (%)	0.82±1.22	1.65±0.68	0.37

Bpm indicates beats per minute; MI, myocardial infarction; PVC, premature ventricular complex; VTE, ventricular tachyarrhythmic event.

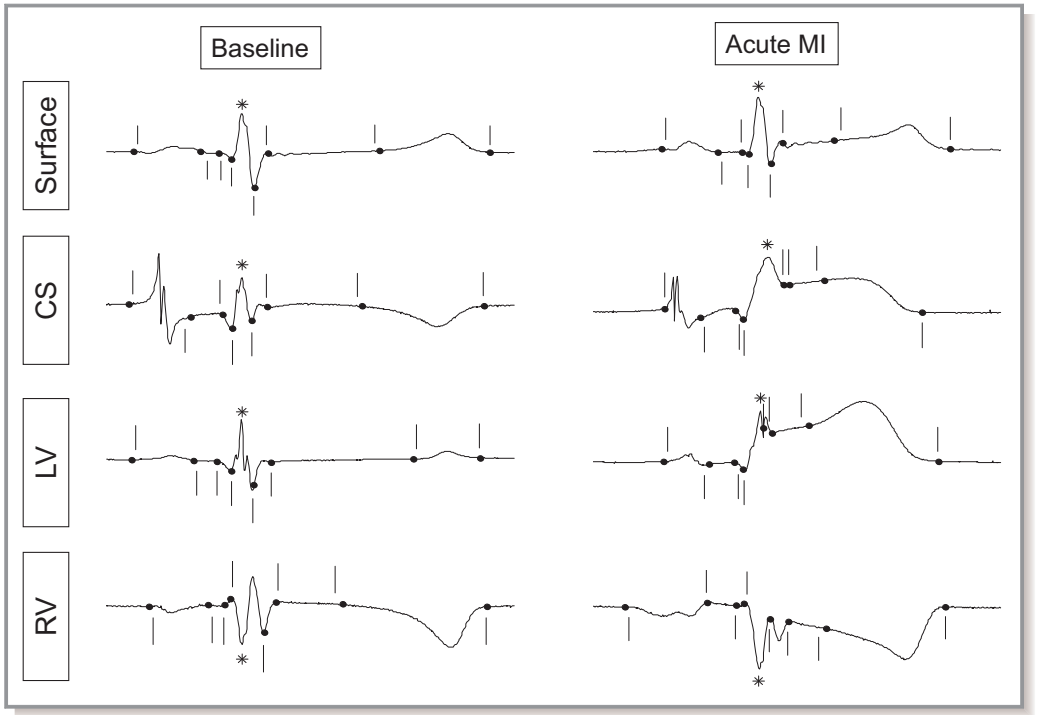

Figure 1. Representative body-surface and intracardiac electrocardiographic beats at baseline (left panels) and during acute myocardial ischemia (MI, right panels). The manual annotations (averaged for 2 independent reviewers) are shown by vertical lines, and the corresponding wavelet delineation results are depicted by circles. Asterisks indicate R waves. CS indicates coronary sinus; LV, left ventricle; RV, right ventricle.

accounts for changes in both ventricular depolarization and repolarization would be a sensitive marker of acute ischemia, especially for intracardiac electrograms.

To assess the intrasubject variability of the ischemic index, we split the baseline recording in 2 parts and computed the SD of the ischemic index for each subject and lead in the first and second halves of the recording. We then quantified the intrasubject variability as the difference between the 2 SDs. A 1-sample *t* test was applied to the differences evaluated for each lead across the whole set of subjects. The estimated *P* values for the body-surface, CS, LV, and RV leads were 0.56, 0.96, 0.45, and 0.17, respectively, indicating that the ischemic index has significantly low intrasubject variability and presents high stability during a baseline recording, thus providing a reliable reference for the evaluation of ischemia-induced changes.

We further evaluated the intersubject variability by comparing the difference between the aforementioned 2 SDs with the SD of the overall variability across all subjects. We used a 1-sample *t* test to compare the intrasubject variability to the intersubject variability of the whole population for each of the body surface and intracardiac leads. The *P* values for the body surface, CS, LV, and RV leads were computed as 0.93, 0.95, 0.46, and 0.16, respectively. These results indicate that, across all leads, there is not a statistically significant difference of the ischemic index between intrasubject variability and the SD of the whole baseline across subjects. Consequently, we conclude that the intra- and intersubject variability of the ischemic index is small, making it a reliable index for the quantification of post-MI changes across different subjects.

Dynamic Changes of Ischemic Index During Myocardial Infarction

Temporal changes of the ischemic index measured at the last minute of baseline prior to balloon inflation and following coronary occlusion were computed for the body-surface and unipolar intracardiac leads at different time bins, with a 30-second resolution for the first 5 minutes after occlusion and a 1-minute resolution afterward. We also created far-field bipolar signals obtained from leads in the RV and CS.[17] Figure 3 shows the dynamic changes of ischemic index at baseline and during MI for body-surface, unipolar, and bipolar intracardiac signals (n=17).

We observe that the ischemic index increases after the onset of ischemia and that the ischemia-induced changes are detectable on unipolar and bipolar intracardiac leads as well as on body-surface leads; however, the timing of the ischemia-induced changes is different across body-surface

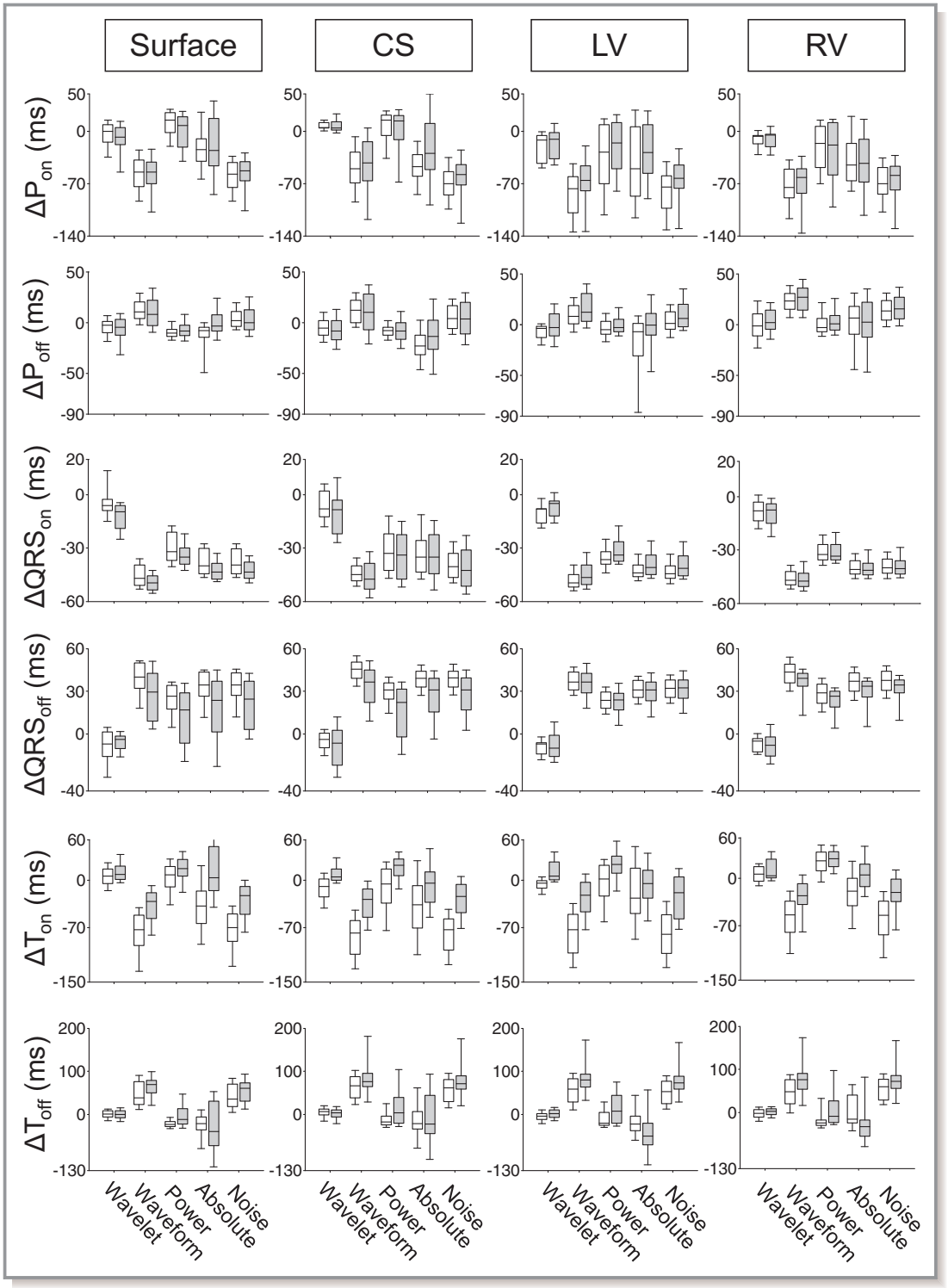

Figure 2. Comparison of methods used for body-surface and intracardiac ECG delineation. The distribution of differences between manual annotations (averaged for 2 independent reviewers) and those obtained by the wavelet-transform, waveform, power, absolute, and noise methods are presented for the onset and offset of P wave, QRS complex, and T wave. Each set of differences has been shown at baseline (white boxes) and following coronary balloon occlusion (gray boxes) for body surface and intracardiac CS, LV, and RV leads. Data are presented as median (horizontal solid line), 25th to 75th percentiles (box) and 10th to 90th percentiles (error bars). For each point and each lead, the wavelet annotations provide the smallest difference from the manually identified reference points. CS indicates coronary sinus; LV, left ventricle; RV, right ventricle.

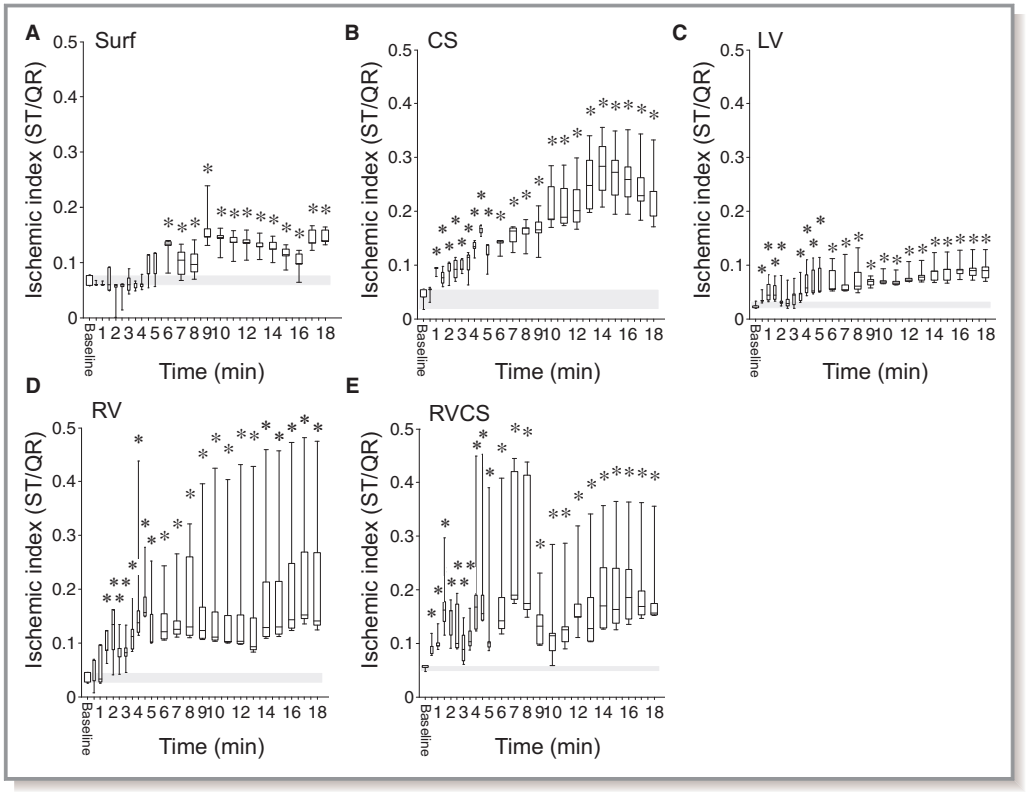

Figure 3. Dynamic changes of ischemic index (n=17) at baseline and following myocardial infarction (MI) in body surface (A), unipolar intracardiac coronary sinus (CS) (B), left ventricle (LV) (C), right ventricle (RV) (D), and triangular RV-CS (E) leads. For each time bin, the distribution of ischemic index is averaged for all study subjects. The time bin width is 1 minute for baseline, 30 seconds for the first 5 minutes following balloon occlusion, and 1 minute for 5 to 18 minutes after occlusion. Data are presented as median (horizontal solid line), 25th to 75th percentiles (box) and 10th to 90th percentiles (error bars). The limits of the distribution of ischemic index at baseline are shown with a gray box throughout the time course of MI to provide a visual means of comparing the one directional significance at each time bin. All ischemic index distributions that are statistically greater than the baseline ischemic index distributions are indicated by asterisks (all $P<0.0022$).

and intracardiac leads. Statistical comparison of the distribution of ischemic index at each time bin during occlusion to that at baseline reveals that the body-surface leads have the largest duration to detection because the earliest significant change is identified after 6 minutes ($P<0.0022$ at all statistically significant time bins). For intracardiac leads, the timing for the occurrence of significant changes varied with lead type, ranging from 30 to 90 seconds after initiation of coronary occlusion ($P<0.0002$ for CS, $P<0.0016$ for LV, $P<0.0020$ for RV, $P<0.0011$ for RV-CS, at all statistically significant time bins). In particular, we found that the triangular RV-CS lead configuration offers the smallest duration to detection of the onset of acute ischemia (30 seconds; $P<0.0011$) partly due to the broader 3-dimensional view of the myocardium and a wider solid angle to the heart when compared with unipolar leads from intracardiac catheters.

In summary, these results support the hypothesis that the ischemia-induced morphologic changes are most prominently seen in intracardiac leads. Of note, we observed that the ischemic index remained stably and significantly elevated during coronary balloon occlusion.

Temporal Analysis of Ischemia Detection in Body-Surface and Intracardiac Signals

To examine the time to ischemia detection using body-surface and intracardiac signals and to investigate whether ischemia detection using intracardiac leads improves the probability of ischemia detection compared with body-surface electrograms alone, for each time bin, we estimated the conditional probabilities of a significant change (from baseline to postocclusion) in the ischemic index for body surface, given a significant change in the ischemic index measured from an intracardiac lead (n=17).

In Figure 4A (left axis), we plot the probability that the change in ischemic index from baseline to postocclusion detected on a body-surface lead is significant given that the

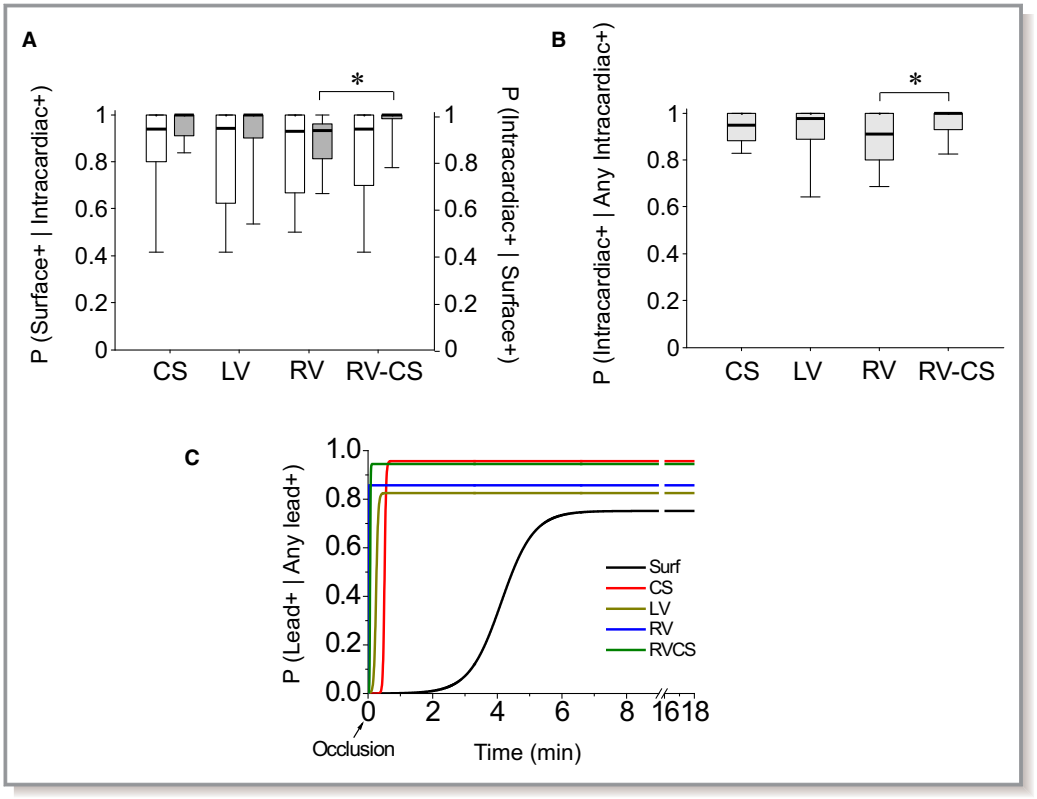

Figure 4. Acute ischemia detection in body-surface ECGs versus intracardiac electrograms (n=17). (A) Probability of observing a statistically significant change in a body-surface lead given a statistically significant change in the corresponding intracardiac lead for each of the coronary sinus (CS), left ventricle (LV), right ventricle (RV), and triangular RV-CS intracardiac lead configurations (left axis, white box plots) versus the probability of observing a statistically significant change in an intracardiac CS, LV, RV, or RV-CS lead given that the change in the corresponding body surface lead is statistically significant (right axis, gray box plots). For all intracardiac leads, the probability of observing a significant change in an intracardiac lead given a significant change in a body-surface lead is always higher than the probability of observing a significant change in a body-surface lead given a significant change in an intracardiac lead ($P<0.0381$). Furthermore, the probability of observing a significant change in RV-CS given a significant change in a body-surface lead is significantly higher than the probability of observing a significant change in RV ($P<0.0158$). No statistical difference was found between any other 2 leads. (B) The probability of observing a significant change in an intracardiac lead configuration given that a significant change has been observed in at least one intracardiac lead for each of the CS, LV, RV, and triangular RV-CS lead configurations. The RV-CS probability was found to be significantly larger than RV probability ($P<0.0415$). No statistical difference was found between any other 2 leads. (C) Conditional probability (as a function of time) that the ischemic index following MI exceeds 3 SDs of its baseline value given that a 3 SD increase has been observed in any other lead configuration (body surface, CS, LV, RV, and RV-CS). Data are presented as median (horizontal solid line), 25th to 75th percentiles (box), and 10th to 90th percentiles (error bars). *$P<0.05$.

change in ischemic index following balloon inflation is significantly higher in an intracardiac lead from each of the CS, LV, RV, and triangular RV-CS lead configurations (quantified across all time bins). The probability (across subjects) that the change measured from a body-surface lead is significant is 0.81 ± 0.27 when a CS lead shows a significant change in the ischemic index, 0.80 ± 0.28 when an LV lead indicates a significant change, 0.80 ± 0.27 when an RV lead shows a significant change, and 0.80 ± 0.27 when a lead from the triangular RV-CS configuration shows a significant increase in the ischemic index from baseline to postocclusion.

To explore the probability of ischemia detection using intracardiac signals, in Figure 4A (right axis), we plot the probability that the change in ischemic index from baseline to postocclusion detected on an intracardiac lead configuration is significant given that the change in ischemic index measured from the body surface is significantly higher after occlusion than at baseline for each of the CS, LV, RV, and triangular RV-CS lead configurations (quantified across all time bins). When the change of the ischemic index from baseline to postocclusion in a body-surface lead is significant, the probability that an intracardiac lead shows a significant

change in the ischemic index is 0.95±0.07 for CS, 0.90±0.17 for LV, 0.96±0.08 for RV, and 0.88±0.12 for the triangular RV-CS configuration.

Compared with the detection probabilities of body-surface leads, we observed average improvement of 14%, 10%, 16%, and 8% in the detection probabilities for CS, LV, RV, and RV-CS leads, respectively. The results demonstrate that for all intracardiac leads, the probability of observing a significant change of the ischemic index in an intracardiac lead given a significant change in a body surface lead is always higher than the probability of observing a significant change in a body surface lead given a significant change in an intracardiac lead ($P<0.0381$), suggesting that intracardiac leads have higher likelihood to detect acute ischemia. We found that the probability of observing a significant change in RV-CS given a significant change in a body surface lead is significantly higher than the probability of observing a significant change in RV ($P<0.0158$). No statistical difference was found between any other 2 leads.

To examine which intracardiac-lead combination has a higher probability of detecting ischemia-induced changes, in Figure 4B, we plot the probability of observing a significant change in an intracardiac lead configuration given that a significant change has been observed in at least 1 intracardiac lead for each of the CS, LV, RV, and triangular RV-CS lead configurations. We notice that the average probability that a triangular RV-CS lead is positive is 0.96, that is, greater than any other intracardiac lead configuration. Of note, the RV-CS probability was significantly larger than the RV configuration ($P<0.0415$). No statistical difference was found between any other 2 leads.

Finally, to assess the time-dependent likelihood of each lead to detect ischemia-induced changes, in Figure 4C, we plot the conditional probability (as a function of time averaged over subjects) of observing an increase in the ischemic index exceeding 3 SD from each subject's ischemic index at baseline[16] given that a shift beyond 3 SD has been observed in any lead for each of the body-surface, CS, LV, RV, and RV-CS lead configurations. The data are presented as sigmoidal fit with the Boltzmann equation ($y=A_2+(A_1-A_2)/(1+\exp((x-x_o)/dx))$, in which A_1 and A_2 represent the minimum and maximum probability, respectively; x_o represents the time to half maximum probability; and dx represents the slope of the exponential function). To fit the model to the postocclusion data only, we deployed a constrained nonlinear optimization subject to $x_o-5dx>0$ to force the sigmoid rise to begin after the start of occlusion.

Using this method, we obtained transition times of 398, 38, 25, 2, and 6 seconds and maximum probability of 0.75, 0.96, 0.83, 0.86, and 0.95 for body-surface, CS, LV, RV, and RV-CS leads, respectively. Putting these results together, the RV-CS lead-configuration system provides the most accurate and rapid detection of ischemia-induced changes compared with baseline than any other lead system.

The Ischemic Index During the 24-Hour Period Following Myocardial Infarction

We used 24-hour Holter, 12-lead ECG signals (n=4) to estimate the ischemic index at baseline (before MI) and following MI. For each subject, the median ischemic index was obtained every 1 hour during baseline and post-MI recordings. Figure 5 shows the overall distribution of ischemic index at baseline and during the 24 hours following MI.

Using mixed-model linear regression to assess the temporal changes of ischemic index from baseline to the 24-hour phase after MI, we found a statistically significant increase in lead I, aVR, and all precordial leads ($P<0.0388$). We observed a marginally significant increase in aVL ($P<0.0523$) and aVF ($P<0.0607$). No statistically significant change from baseline to 24-hour recording after MI was observed in other leads.

Temporal Analysis of Ischemic Index Preceding Ventricular Tachyarrhythmic Events

To expand the prognostic value of the ischemic index beyond short-term prediction of acute MI, we sought to assess its utility in predicting VTEs.

We estimated the ischemic index before a VTE (n=9) during the acute phase of MI. In Figure 6, we show the distribution of the ischemic index in body-surface, unipolar, and bipolar intracardiac signals up to 12 minutes before the onset of VTEs. In body-surface leads, the ischemic index presented a significant surge (compared with a baseline before occlusion) 2 minutes prior to the event ($P<0.0464$) and remained marginally significant immediately before VTE ($P<0.0927$). Compared with baseline, intracardiac ischemic index before the onset of VTE was found to be significantly higher during the last 2 minutes in CS ($P<0.0022$), the last 6 minutes in LV ($P<0.0464$), the last minute in RV ($P<0.0360$), and the last 2 minutes in RV-CS ($P<0.0055$). Of note, the earliest significant surge in the ischemic index was observed 12 minutes before the onset of VTE in RV-CS leads.

We further sought to probe the prognostic role of ischemic index in a 12-lead ECG Holter recording of a subject that experienced sudden cardiac death during the first 24 hours after MI. In Figure 7, we present the dynamic changes of the ischemic index during baseline (24-hour Holter recording before MI induction) and the 13-hour phase after MI until sudden cardiac death. The results obtained during the acute phase of MI show sustained elevation of the ischemic index that remains significantly higher than baseline for 3 hours after MI ($P<0.0001$) and is significantly higher during the 2nd to 11th hours of follow-up ($P<0.0001$). In addition, the

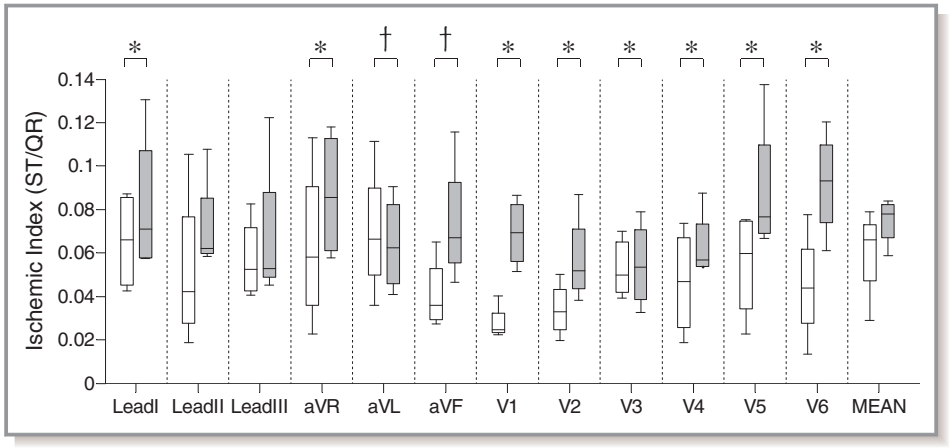

Figure 5. The ischemic index estimated from 24-hour Holter ECG recordings at baseline and immediately after myocardial infarction (MI; n=4). For each subject, the median ischemic index estimated every hour during baseline was compared with its corresponding value after MI. Linear mixed-effects model regression showed a statistically significant (*P<0.05) increase in lead I, aVR, and all precordial leads (P<0.0388) and a marginally significant (†0.05<P<0.1) increase in aVL (P<0.0523) and aVF (P<0.0607). Data are presented as median (horizontal solid line), 25th to 75th percentiles (box), and 10th to 90th percentiles (error bars).

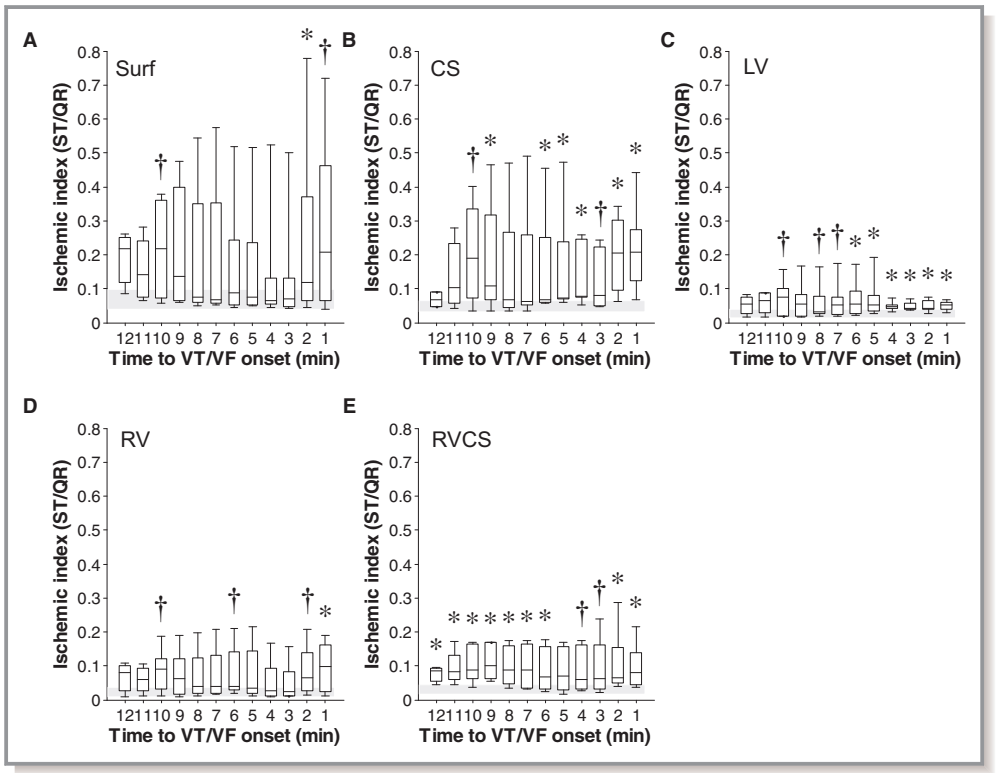

Figure 6. Dynamic changes of ischemic index preceding ventricular tachyarrhythmic events (n=9) in body surface (A), unipolar intracardiac coronary sinus (CS) (B), left ventricle (LV) (C), right ventricle (RV) (D), and triangular RV-CS (E) leads in the animal model of acute myocardial infarction. The ischemic index before the onset of ventricular tachyarrhythmic events was found to remain significantly higher than baseline during the last 2 minutes in CS (P<0.0022), the last 6 minutes in LV (P<0.0464), the last minute in RV (P<0.0360), and the last 2 minutes in RVCS (P<0.0055). In body-surface leads, the ischemic index presented a significant surge 2 minutes prior to the event (P<0.0464) and remained marginally significant immediately before ventricular tachyarrhythmic events (P<0.0927). *P<0.05; †0.05<P<0.1. Data are presented as median (horizontal solid line), 25th to 75th percentiles (box), and 10th to 90th percentiles (error bars). CS indicates coronary sinus; LV, left ventricle; RV, right ventricle.

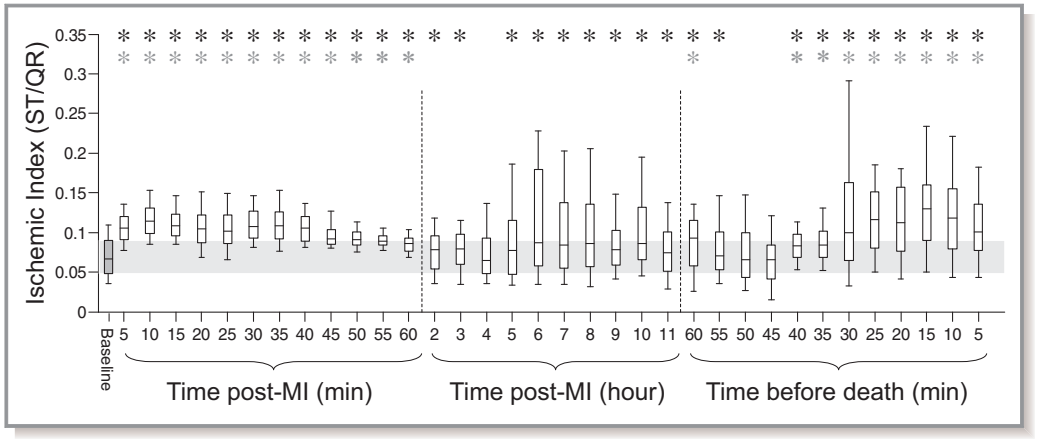

Figure 7. Temporal changes of the ischemic index following myocardial infarction (MI) compared with baseline (n=1) until sudden cardiac death. The results demonstrate sustained elevation of the ischemic index during the first hour after MI that remains significantly higher than baseline for 3 hours after MI ($P<0.0001$; black asterisk), and the value of the ischemic index becomes significantly lower during the 2nd to 11th hours after MI ($P<0.0001$; gray asterisk). Specifically, the ischemic index shows a significant increase 40 minutes before sudden cardiac death ($P<0.0001$ compared to baseline, black asterisk; $P<0.0001$ compared with the value of the ischemic index during the 2nd to 11th hours after MI; gray asterisk). Data are presented as median (horizontal solid line), 25th to 75th percentiles (box), and 10th to 90th percentiles (error bars).

ischemic index demonstrates a significant increase 40 minutes before death ($P<0.0001$ compared with baseline). Of note, comparison of the ischemic index during the 2nd to 11th hours after MI with baseline, showed a significant increase 40 minutes prior to the event ($P<0.0001$).

Taken together, these findings suggest that an increase in the ischemic index may play an important prognostic role in the early detection of a VTE. Specifically, monitoring the intracardiac ischemic index from the triangular RV-CS leads may provide earlier prediction of the impending arrhythmia onset.

Discussion

Early identification of acute MI and prompt intervention may help improve clinical outcomes. Body-surface ECG monitoring is most commonly used to detect MI; however, it is less sensitive to coronary artery events than intracardiac electrograms.[9,10] In contrast, ST-segment changes in intracardiac electrograms have been shown to produce early warnings of coronary occlusion associated with a median alert-to-door time of 19.5 minutes for patients at high risk of recurrent coronary syndromes, who otherwise present with delays of 2 to 3 hours.[16] These observations demonstrate the potential capacity of intracardiac signals to predict early onset of acute ischemia and to deliver timely therapy either through an implantable device or at a medical facility.

This study presents a comprehensive and systematic demonstration of the utility of a novel method to monitor the ischemia-induced changes in intracardiac and body-surface signals. First, we propose a wavelet-based approach for the accurate delineation of characteristic points in intracardiac electrograms that is in excellent agreement with the manually delineated electrograms and is robust to ischemia-induced changes during MI. Second, we introduce an index to quantify beat-to-beat changes observed in both ventricular depolarization and repolarization during ischemia; the index normalizes the ST height to the QR amplitude so as to provide a normalized subject- and lead-independent measure that accounts for both depolarization[31,32] and repolarization[3–5] changes in the presence of MI. Third, despite the dynamic beat-to-beat and subject-to-subject variability of ECG morphology, our data indicate that the ischemic index presents high stability as well as very low intra- and intersubject variability under baseline (nonischemic) conditions. Fourth, estimation of the ischemic index from intracardiac signals provides a highly efficient and accurate means of detecting the onset of an acute ischemic episode or the progression of an ongoing ischemic episode. Fifth, the intracardiac leads exhibit greater ability to detect MI-induced changes compared with body surface ECGs. Sixth, the ischemic index may serve as a predictor of VTEs.

Recent clinical studies investigating the predictive role of intracardiac electrograms to detect life-threatening ventricular arrhythmias[25] or flow-limiting coronary obstruction[16] have successfully demonstrated that intracardiac ST-segment monitoring can predict arrhythmic events. Specifically, Fischell et al[16] reported early detection of the presence of acute MI in patients at high risk for acute coronary syndromes. Consistent with these findings, our results showed that

monitoring the ischemic index can reliably predict the onset of ischemia in intracardiac signals. In the whole study population, the first statistically significant change of ischemic index in body-surface leads was observed 6 minutes after balloon inflation, whereas the unipolar intracardiac electrograms offered a significant change as early as 30, 60, and 90 seconds for LV, CS, and RV leads, respectively. Beyond the setting of acute coronary syndromes, our data also suggest that intracardiac detection of ischemia may play an important role in the diagnosis and treatment of patients with "silent" ischemia, which is likely underdiagnosed due to the lack of effective screening tools and has been associated with adverse clinical outcomes.[33]

We further observed that adopting the triangular intracardiac lead configuration between the RV and CS catheters provided the smallest duration in detecting the onset of acute ischemia, that is, within 30 seconds after balloon occlusion of the coronary artery ($P<0.0011$). This improvement (manifested by a lower P value) may be due to the fact that RV-CS lead configuration provides a broader 3-dimensional view of myocardium and better localization of the ischemic event. In addition, our results showed that in the acute stage of MI, the probability of observing a significant change in an intracardiac lead given a significant change in a body-surface lead is always higher than the probability of observing a significant change in a body-surface lead given a significant change in an intracardiac lead ($P<0.0381$).

Assessing the 24-hour changes of ischemic index during the chronic phase after MI showed a statistically significant increase in lead I, aVR, and all precordial leads from baseline to ischemia ($P<0.0388$). Finally, we have been able to demonstrate that ischemic index presents a significant surge preceding VTEs ($P<0.0360$).

In conclusion, our findings support the hypothesis that analysis of intracardiac signals provides early detection of ischemia-induced electrocardiographic changes that exhibit higher sensitivity than body-surface ECGs in determining the onset of ischemia. Furthermore, monitoring the ischemic index may present a potentially useful method in predicting ischemia-induced VTEs. In view of the options of currently available implantable cardioverter defibrillators, monitoring of the proposed intracardiac ischemic index may be a potentially clinically feasible means of alert regarding early onset of acute ischemia associated with thrombotic occlusion in patients at high risk for recurrent coronary syndromes and may provide an early trigger of appropriate medical therapy.

Study Limitations

A limitation of the presented methodology, which uses the WT to obtain ECG annotations to estimate the ischemic index, is that it is defined for normal beats only; however, this limitation is inherent to all methods that rely on processing the morphology of ECG signals. Moreover, a complete receiver operating curve analysis should be performed in a study with a sufficiently large number of subjects to ensure adequate power in establishing diagnostic ischemic index thresholds and to assess the sensitivity and specificity of the proposed method.

Sources of Funding

This work was supported by a Scientist Development Grant (0635127N), a Founders Affiliate Postdoctoral Fellowship (12POST9310001) from the American Heart Association, the Kenneth M. Rosen Fellowship in Cardiac Pacing and Electrophysiology (13-FA-32-HRS) from the Heart Rhythm Society, and by NIH grant 1R21AG035128. This work was also supported by a Fellowship and a Science Award from the Center for Integration of Medicine and Innovative Technology (CIMIT), by the Spanish government (MINECO) and European Union (FEDER) under projects TEC2010-21703-C03-02 and TEC2013-42140-R and by the European Social Fund and the Aragon government under Grupo Consolidado BSICoS. This work was conducted with support from Harvard Catalyst, The Harvard Clinical and Translational Science Center (National Center for Research Resources and the National Center for Advancing Translational Sciences, National Institutes of Health Award 8UL1TR000170-05 and financial contributions from Harvard University and its affiliated academic health care centers).

Disclosures

None.

References

1. Myerburg RJ, Kessler KM, Castellanos A. Sudden cardiac death. Structure, function, and time-dependence of risk. *Circulation*. 1992;85:I2–10.
2. Solomon SD, Zelenkofske S, McMurray JJ, Finn PV, Velazquez E, Ertl G, Harsanyi A, Rouleau JL, Maggioni A, Kober L, White H, Van de Werf F, Pieper K, Califf RM, Pfeffer MA. Sudden death in patients with myocardial infarction and left ventricular dysfunction, heart failure, or both. *N Engl J Med*. 2005;352:2581–2588.
3. Shah A, Wagner GS, Granger CB, O'Connor CM, Green CL, Trollinger KM, Califf RM, Krucoff MW. Prognostic implications of TIMI flow grade in the infarct related artery compared with continuous 12-lead ST-segment resolution analysis. Reexamining the "gold standard" for myocardial reperfusion assessment. *J Am Coll Cardiol*. 2000;35:666–672.
4. Krucoff MW, Croll MA, Pope JE, Pieper KS, Kanani PM, Granger CB, Veldkamp RF, Wagner BL, Sawchak ST, Califf RM. Continuously updated 12-lead ST-segment recovery analysis for myocardial infarct artery patency assessment and its correlation with multiple simultaneous early angiographic observations. *Am J Cardiol*. 1993;71:145–151.
5. Holland RP, Brooks H. TQ-ST segment mapping: critical review and analysis of current concepts. *Am J Cardiol*. 1977;40:110–129.
6. Myocardial infarction redefined–a consensus document of The Joint European Society of Cardiology/American College of Cardiology Committee for the redefinition of myocardial infarction. *Eur Heart J*. 2000; 21:1502–1513.

7. Schroder K, Wegscheider K, Zeymer U, Tebbe U, Schroder R. Extent of ST-segment deviation in a single electrocardiogram lead 90 min after thrombolysis as a predictor of medium-term mortality in acute myocardial infarction. *Lancet*. 2001;358:1479–1486.
8. Menown IB, Mackenzie G, Adgey AA. Optimizing the initial 12-lead electrocardiographic diagnosis of acute myocardial infarction. *Eur Heart J*. 2000; 21:275–283.
9. Fischell TA, Fischell DR, Fischell RE, Baskerville S, Hendrick S, Moshier C, Harwood JP, Krucoff MW. Potential of an intracardiac electrogram for the rapid detection of coronary artery occlusion. *Cardiovasc Revasc Med*. 2005;6:14–20.
10. Siegel S, Brodman R, Fisher J, Matos J, Furman S. Intracardiac electrode detection of early or subendocardial ischemia. *Pacing Clin Electrophysiol*. 1982;5:892–902.
11. Shenasa M, Hamel D, Nasmith J, Nadeau R, Dutoy JL, Derome D, Savard P. Body surface potential mapping of ST-segment shift in patients undergoing percutaneous transluminal coronary angioplasty. Correlations with the ECG and vectorcardiogram. *J Electrocardiol*. 1993;26:43–51.
12. Rautaharju PM, Surawicz B, Gettes LS, Bailey JJ, Childers R, Deal BJ, Gorgels A, Hancock EW, Josephson M, Kligfield P, Kors JA, Macfarlane P, Mason JW, Mirvis DM, Okin P, Pahlm O, van Herpen G, Wagner GS, Wellens H. AHA/ACCF/HRS recommendations for the standardization and interpretation of the electrocardiogram: part IV: the ST segment, T and U waves, and the QT interval: a scientific statement from the American Heart Association Electrocardiography and Arrhythmias Committee, Council on Clinical Cardiology; the American College of Cardiology Foundation; and the Heart Rhythm Society. Endorsed by the International Society for Computerized Electrocardiology. *J Am Coll Cardiol*. 2009;53:982–991.
13. Barnard RJ, Buckberg GD, Duncan HW. Limitations of the standard transthoracic electrocardiogram in detecting subendocardial ischemia. *Am Heart J*. 1980;99:476–482.
14. Chaitman BR, Bourassa MG, Wagniart P, Corbara F, Ferguson RJ. Improved efficiency of treadmill exercise testing using a multiple lead ECG system and basic hemodynamic exercise response. *Circulation*. 1978;57:71–79.
15. Myerburg RJ. Implantable cardioverter-defibrillators after myocardial infarction. *N Engl J Med*. 2008;359:2245–2253.
16. Fischell TA, Fischell DR, Avezum A, John MS, Holmes D, Foster M III, Kovach R, Medeiros P, Piegas L, Guimaraes H, Gibson CM. Initial clinical results using intracardiac electrogram monitoring to detect and alert patients during coronary plaque rupture and ischemia. *J Am Coll Cardiol*. 2010;56:1089–1098.
17. Weiss EH, Merchant FM, d'Avila A, Foley L, Reddy VY, Singh JP, Mela T, Ruskin JN, Armoundas AA. A novel lead configuration for optimal spatio-temporal detection of intracardiac repolarization alternans. *Circ Arrhythm Electrophysiol*. 2011; 4:407–417.
18. Wilber DJ, Garan H, Ruskin JN. Electrophysiologic testing in survivors of cardiac arrest. *Circulation*. 1987; 75:III146–153.
19. Laguna P, Jane R, Caminal P. Automatic detection of wave boundaries in multilead ECG signals: validation with the CSE database. *Comput Biomed Res*. 1994;27:45–60.
20. Merri M, Alberti M, Benhorin J, Hall WJ, Locati E, Moss AJ, eds. Quantitation of ventricular repolarization: a new approach. In: Proc. *Computers in Cardiology*, 1988: 85–87.
21. Laguna P, Thakor NV, Caminal P, Jane R, Yoon HR, Bayes de Luna A, Marti V, Guindo J. New algorithm for QT interval analysis in 24-hour Holter ECG: performance and applications. *Med Biol Eng Comput*. 1990;28:67–73.
22. de Chazal P, Celler BG. Automatic measurement of the QRS onset and offset in individual ECG leads. in Proc. EMBS. 1996; 1399–1400.
23. Mallat S. A theory for multiresolution signal decomposition: the wavelet representation. *IEEE, Trans Pattern Anal Mach Intell*. 1989;11:674–693.
24. Martínez JP, Almeida R, Olmos S, Rocha AP, Laguna P. A wavelet-based ECG delineator: evaluation on standard databases. *IEEE Trans Biomed*. 2004;51:570–581.
25. Tereshchenko LG, McCabe A, Han L, Sur S, Huang T, Marine JE, Cheng A, Spragg DD, Sinha S, Calkins H, Stein K, Tomaselli GF, Berger RD. Intracardiac J-point elevation before the onset of polymorphic ventricular tachycardia and ventricular fibrillation in patients with an implantable cardioverter-defibrillator. *Heart Rhythm*. 2012;9:1594–1602.
26. Abboud S, Smith JM, Shargorodsky B, Laniado S, Sadeh D, Cohen RJ. High frequency electrocardiography of three orthogonal leads in dogs during a coronary artery occlusion. *Pacing Clin Electrophysiol*. 1989;12: 574–581.
27. Abboud S, Cohen RJ, Sadeh D. A spectral analysis of the high frequency QRS potentials observed during acute myocardial ischemia in dogs. *Int J Cardiol*. 1990;26:285–290.
28. Abboud S, Cohen RJ, Selwyn A, Ganz P, Sadeh D, Friedman PL. Detection of transient myocardial ischemia by computer analysis of standard and signal-averaged high-frequency electrocardiograms in patients undergoing percutaneous transluminal coronary angioplasty. *Circulation*. 1987;76: 585–596.
29. Pettersson J, Pahlm O, Carro E, Edenbrandt L, Ringborn M, Sornmo L, Warren SG, Wagner GS. Changes in high-frequency QRS components are more sensitive than ST-segment deviation for detecting acute coronary artery occlusion. *J Am Coll Cardiol*. 2000;36:1827–1834.
30. Lee YZ, Belk PA, Mullen TJ, Rivers S, Zhang X, Armoundas AA, Osaka M, He B, Aldea G, Cohen RJ. Comparison of body surface potential and laplacian mapping with epicardial mapping for detection of cardiac ischemia in pigs. *Ann Noninvasive Electrocardiol*. 1998;3:244–251.
31. Ringborn M, Pettersson J, Persson E, Warren SG, Platonov P, Pahlm O, Wagner GS. Comparison of high-frequency QRS components and ST-segment elevation to detect and quantify acute myocardial ischemia. *J Electrocardiol*. 2010;43:113–120.
32. Romero D, Ringborn M, Laguna P, Pahlm O, Pueyo E. Depolarization changes during acute myocardial ischemia by evaluation of QRS slopes: standard lead and vectorial approach. *IEEE Trans Biomed Eng*. 2011;58:110–120.
33. Conti CR, Bavry AA, Petersen JW. Silent ischemia: clinical relevance. *J Am Coll Cardiol*. 2012;59:435–441.